JOURNAL OF PROTEOMICS 74 (2011) 186–198

available at www.sciencedirect.com

ScienceDirect

www.elsevier.com/locate/jprot

Characterization of the B-Raf interactome in mouse hippocampal neuronal cells

Juan J. Bonfiglio[a,1], *Giuseppina Maccarrone*[b,1], *Christiane Rewerts*[b], *Florian Holsboer*[b], *Eduardo Arzt*[a], *Christoph W. Turck*[b], *Susana Silberstein*[a,*]

[a]*Laboratorio de Fisiología y Biología Molecular, Departamento de Fisiología y Biología Molecular y Celular, Facultad de Ciencias Exactas y Naturales (FCEN), Universidad de Buenos Aires, and IFIBYNE-CONICET, Buenos Aires, Argentina*
[b]*Max Planck Institute of Psychiatry, Kraepelinstrasse 2-10, 80804 Munich, Germany*

ARTICLE INFO

Article history:
Received 24 September 2010
Accepted 20 October 2010

Keywords:
B-Raf
Interactome
Mass spectrometry
Neurons
Proteomics

ABSTRACT

B-Raf links a variety of extracellular stimuli downstream of cell surface receptors, constituting a determining factor in the ability of neurons to activate ERK. A detailed study of the B-Raf interactome is necessary to clarify the intricacy of B-Raf-dependent signal transduction. We used a mouse hippocampal cell line (HT22) that expresses B-Raf at high levels, to identify B-Raf associated proteins under endogenous expression conditions, avoiding artificial interactions from overexpression studies. We used stringent procedures to co-immunoprecipitate proteins that specifically associate with endogenous B-Raf with the help of gel electrophoresis separation and off-line LC-MALDI-MS/MS proteomic analysis. Our stringent protein identification criteria allowed confident identification of B-Raf interacting proteins under non-stimulating conditions. The presence of previously reported B-Raf interactors among the list of proteins identified confirms the quality of proteomic data. We identified tubulin and actin as B-Raf interactors for the first time, among structural and accessory proteins of cell cytoskeleton, molecular chaperones (Hsc70, GRP78), and cellular components involved in aspects of mRNA metabolism and translation. Interactions were validated in HT22 cells and in the neuronal cell line Neuro-2a providing further evidence that the identified proteins are B-Raf interactors, which constitute a basis for understanding MAPK pathway regulation in neurons.

1. Introduction

The Raf/MAPK kinase/extracellular-signal-regulated kinase cascade links a variety of extracellular stimuli, acting through cell surface receptors, to the regulation of several cellular processes including proliferation, survival and differentiation [1]. Raf activation is initiated by RAS-GTP association with the RAS binding domain (RBD) of this kinase. Concomitant conformational changes and recruitment to the cell membrane promote changes in Raf phosphorylation that combine to stimulate its serine/threonine kinase activity, triggering sequential phosphorylation and activation of MEK and ERK [2,3].

The Raf family in mammals includes three members: A-Raf, B-Raf, and C-Raf/Raf-1. The three Raf proteins share three conserved regions (CR). CR1 and CR2 are located in the

Abbreviations: IP, immunoprecipitation; ERK, extracellular-signal-regulated kinase; MAPK, mitogen-activated protein kinase; MEK, MAPK/ERK kinase; MAPKKK, MAPK kinase kinase.

* *Corresponding author*. Tel.: +54 11 4576 3368/86; fax: +54 11 4576 3321.
E-mail address: ssilberstein@fbmc.fcen.uba.ar (S. Silberstein).

[1] These authors contributed equally to this work.

1874-3919/$ – see front matter © 2010 Elsevier B.V. All rights reserved.
doi:10.1016/j.jprot.2010.10.006

regulatory N-terminus, whereas CR3 corresponds to the C-terminus catalytic kinase domain [4]. Other regions more divergent are supposed to account for the differences found in the regulation and function of the Raf family members [5]. Raf isoforms display different abilities to phosphorylate and activate MEK1 and MEK2, with B-Raf being the most active, followed by Raf-1 and then A-Raf [6,7]. In many cell types B-Raf appears to constitute the majority of detectable MEK kinase activity [8–11]. These findings, coupled with the normal ERK activation kinetics displayed in A-Raf or Raf-1 knockout mice, suggest that B-Raf may be the most important Raf family member in the ERK activation cascade [12–14]. Furthermore, since – unlike the ubiquitous Raf-1 – B-Raf is predominantly expressed in the nervous system [15], it constitutes a determining factor in the ability of neurons to activate ERK [16]. ERK activity in the central nervous system is linked to a variety of crucial molecular processes [17] and, in limbic areas, it was found to be modulated under different stress-related conditions *in vivo* [18,19].

More than 30 mutations in B-Raf have been associated with human cancers [20,21]. The most common B-Raf mutation ($BRAF^{V600E}$) results in a constitutively active enzyme [22]. The discovery that a single point mutation can impart full catalytic activity to B-Raf suggests that the activation mechanism of B-Raf is distinct from that of Raf-1 and A-Raf, which cannot be activated in this manner [23].

Proteins do not act in isolation but engage in complex and dynamic interactions with other proteins to fulfill their diverse cellular roles [24,25]. A precise understanding of biological pathways and molecular mechanisms involved in protein activity regulation relies on the identification and biochemical characterization of the proteins involved in such molecular processes. To get insight into the mechanism of B-Raf activation and in the regulation of ERK activity in neurons, we used an MS-based proteomic analysis to isolate and identify B-Raf-associated proteins. The MS technique applied in the interactome study of a bait protein reveals to be a powerful tool for the identification of proteins interacting with each other [26–28]. Co-immunoprecipitated proteins with endogenous B-Raf were obtained from lysates of HT22 cells, an immortalized mouse hippocampal cell line with neuronal properties [29]. Immunoprecipitates were resolved by 1D-SDS-PAGE, and gel slices were subjected to in-gel tryptic digestion. The resulting proteolytic peptides were analyzed by off-line LC-MALDI-MS/MS, and the B-Raf interactome under non-stimulated conditions is described.

2. Material and methods

2.1. Cell culture

HT22 mouse hippocampal cells were cultured as monolayer in DMEM (Gibco) supplemented with 5% (v/v) fetal calf serum, 4 mM L-glutamine (Sigma), 10 mM Hepes (Sigma), 2,2 g/liter $NaHCO_3$, 100U/ml penicillin (Gibco), and 100 mg/ml streptomycin (Gibco). Neuro-2a mouse neuroblastoma cells were cultured in DMEM supplemented with 10% (v/v) fetal calf serum, 4 mM L-glutamine, 10 mM Hepes, 2,2 g/liter $NaHCO_3$, 100U/ml penicillin, and 100 mg/ml streptomycin. Cell lines were maintained in an incubator at 37 °C in an atmosphere of 5% CO_2.

2.2. Immunoprecipitation

HT22 cells were grown to 70% confluence and serum starved with Opti-MEM media (Gibco) 17 h before being washed with ice-cold PBS and lysed for 2 h at 4°C with modified RIPA buffer (50 mM Tris pH 7,4; 100 mM NaCl; 1 mM EDTA; 1% NP-40) containing a cocktail of protease inhibitors (Roche Molecular Biomedicals). In order to maximize the recovery of the B-Raf-interacting proteins three 10-cm dishes were used (protein concentration of cell extract: 5.5 mg/ml). IP assays were performed at 4°C overnight with rabbit anti-B-Raf antibodies raised against an epitope corresponding to amino acids 12-156 mapping at the N-terminus of B-Raf (Santa Cruz Biotechnology). Immunoprecipitates were collected using Protein A/G plus agarose (Santa Cruz Biotechnology). A pre-clearing step with a commercial polyclonal non-immune rabbit antibody (Santa Cruz Biotechnology) and protein A/G plus agarose (Santa Cruz Biotechnology) was included before performing B-Raf IPs to prevent non-specific protein binding to the anti-B-Raf rabbit polyclonal antibody. Immunoprecipitates were washed once with cold PBS and solubilized according to the analysis performed. Confirmations of interacting proteins by co-IP and western blot analysis were performed with the same protocol except that only one 10-cm dish of HT22 or Neuro-2a cells was used to prepare the lysate. For reciprocal co-IP confirmations antibodies against vimentin (Abcam) and β-tubulin (Santa Cruz Biotechnology) were used.

2.3. One-dimensional gel electrophoresis

B-Raf protein complex isolated by IP was resuspended in SDS-loading buffer (125 mM Tris, 9.2% SDS, 0.4 M DTT, 40% glycerol, 0.001% bromophenol blue), heated at 95 °C and loaded onto a 10% polyacrylamide gel. After electrophoresis, the proteins were stained by Coomassie Brilliant Blue following the manufacturer's protocol (Bio-Rad) and scanned with the densitometer GS-800 using the PDQuest software (Bio-Rad).

2.3.1. In-gel tryptic digestion

Gel lanes were cut in 20 equal slices and distained twice in ACN/20 mM NH_4HCO_3 pH 8.5 (1/1) at 37 °C for 30 min. Gel slices were dried at room temperature and then rehydrated with the addition of 25 mM NH_4HCO_3 and reduced with 10 mM DTT for 30 min at 56 °C in darkness. After removing the supernatant, 55 mM iodoacetamide (IAA) in 25 mM NH_4HCO_3 was added. The reaction of carboxyamidomethylation proceeded for 30 min at RT in darkness. For the enzymatic digestion 200 ng of trypsin in 20 mM NH_4HCO_3 pH 8.5 was added to each slice. The enzymatic reaction occurred at 37 °C overnight. To quench the enzymatic reaction 1% aqueous acetic acid was added. After the digestion, peptides were extracted by incubating each slice with 2% aqueous formic acid/ACN (1/1) at RT for 20 min and then sonicating for 5 min. The extraction procedure was repeated twice. Supernatants were pooled and then dried using a Savant Speedvac Plus SC210A apparatus (Thermo Scientific).

2.3.2. *Off-line LC-MALDI-MS/MS and protein identification*

The extracted peptides were dissolved in 0.3% TFA aqueous solution and separated with a LC system (HP1100, Agilent Technologies) coupled to a robotic spotter (Proteineer FC, Bruker Daltonics). The sample was loaded onto a RP-C18 monolithic column (200 μm i.d x 5 cm, LC-Packings, Dionex) and separated using 0.1% TFA aqueous buffer (Solvent A) and ACN/0.1% TFA (1/1,v/v) organic buffer (solvent B). The peptides were eluted with a linear gradient of solvent B from 10 to 90% in 15 min at flow rate of 4μl/min. The eluted peptides were co-spotted with a MALDI matrix α-cyano-4-hydroxycinnamic acid (HCCA) dissolved in organic solution buffer (88% EtOH:Acetone (2:1, v/v), 10% saturated HCCA solution in ACN/0.1%TFA (3/7, v/v), 1% 100nM $NH_4H_2PO_4$ in aqueous 0.1%TFA, 1% aqueous 10%TFA) onto a steel anchorchip sample target (Bruker Daltonics) in 96 spots at interval time of 8 s. The spots, prior to the MS analysis, were washed with 10 mM ammonium biphosphate solution. Mass spectra were acquired using an Ultraflex I TOF/TOF mass spectrometer (Bruker Daltonics) equipped with a nitrogen laser. The spectra were externally calibrated applying the standard peptides mixture I (Bruker Daltonics). The data acquisition of MS and MS/MS spectra was performed in automatic mode, controlled and monitored by WARP-LC 1.2 software (Bruker Daltonics). The spectra were acquired at 50 Hz in positive reflectron mode, with an acceleration voltage of 25 kV and a resolution of 19,990 FWHM determined for Somatostatin 28 (MW 3147 Da). For MALDI data 300 and 700 shots for MS and MS/MS spectra were, respectively, accumulated. After the acquisition of the MS spectra, a compounds list for the fragmentation analysis was created by the WARP-LC software. The compounds were selected based on the following criteria: minimum signal/noise (S/N) 10, most intensive peak within 5 Da, 150 ppm mass accuracy and exclusion interval of five fractions. The peak lists of the MS and MS/MS spectra were subsequently combined by BioTools software 3.0 (Bruker Daltonics) and sent to Mascot 2.2 (Matrix Science) search algorithm, both softwares are embedded into WARP-LC software package. The identification of the proteins was achieved by searching against SwissProt 15.3 database (uniprot29.05.09), *Mus musculus* as taxonomy specie, trypsin as enzyme, and allowing one missed cleavage site. The methionine oxidation and cysteine carboxyamidomethylation were set as dynamic and static modifications, respectively. The mass accuracies of the precursor and the fragment ions were set 150 ppm and 0.7 Da, respectively. For the peptide identification the MS/MS spectra were searched with the support of Mascot 2.2 [30]. The results with a significance level over 95% were accepted. The protein identifications were considered confident when at least 2 peptides were contained. The proteins reported in this work were identified in two independent experimental replicates. False positive identification rates were evaluated on all data using a random protein database created with the support of a pearl script *decoy.pl* (www.matrixscience.com), random option is specified. False discovery rate (FDR, *percent*) was calculated by dividing the number of passing random peptide hits by the all peptide hits passing the cut-off criteria in the database search.

2.4. 2D-PAGE analysis and in-gel tryptic digestion

The immunoprecipitated B-Raf complex was analyzed by 2D-PAGE as previously described [31]. Briefly, the immunoprecipitated B-Raf complex was solubilized in the isoelectric focusing (IEF) rehydration buffer and applied to an 11 cm Immobilized pH gradient (IPG) 3-10 NL strip (Bio-Rad). The strip was rehydrated for 12 h at 50 V. Focusing was carried out at 500 V initially and then ramped to 10,000 V and completed at 60,000Vh. Prior to second dimension the proteins were carboxyamidomethylated by incubating the strips in equilibration buffer for 15 min followed by 15 min with the same buffer supplemented with 2.5% IAA (Bio-Rad). The strip was applied to 12% SDS gel and run at 50–200 V. After the completion of the run, the gel was fixed in 10% acetic acid, 50% methanol and stained with ProQ Diamond (Molecular Probes) for the specific detection of phosphorylated proteins. ProQ stained gel images were acquired using a fluorescent scanner FX-imager (Bio-Rad). Subsequently, the gels were stained with colloidal Coomassie Brilliant Blue (Sigma) dissolved in 34% methanol, 17% ammonium sulphate and 2% phosphoric acid. All images were analyzed and compared with the help of PDQuest 2D analysis software (Bio-Rad). ProQ and Coomassie images were analyzed separately.

Protein spots visualized after ProQ staining were excised, distained in 20 mM ammonium bicarbonate/ACN (1:1) and air-dried. Each gel spot was digested with 50 ng trypsin dissolved in 5 μl of 1 mM NH_4HCO_3. After overnight digestion at 37 °C, 1 μl of TFA was added to the digest mixture and sonicated. The peptides were extracted by adding 1% TFA/ACN (1/1, v/v) sonicated for 5 min and shacked at 37 °C for 30 min. The extraction procedure was repeated twice. The supernatant was dried and then resuspended in 0.1% TFA prior the MALDI-MS analysis.

2.4.1. *MALDI-MS and protein identification*

For matrix solution preparation, 4-hydroxy-α-cyano-cinnamic acid (HCCA) (Bruker Daltonics) was saturated in TA30 (0.1% TFA/ACN, 2:1 (v/v)). The matrix was diluted into ethanol: acetone (2:1, v:v) mixture. One microliter of the sample was spotted onto a steel anchorchip MALDI target (Bruker Daltonics). After the matrix-sample had completely dried, all spots were washed with 0.1% TFA. Peptide mass fingerprints (PMF) as well as Lift spectra (MS/MS spectra) were acquired automatically using an Ultraflex I MALDI-TOF/TOF mass spectrometer (Bruker Daltonics). The peaks list of the PMF and Lift spectra were combined and searched against the SwissProt 15.3 database (uniprot29.05.09), taxonomy *Mus musculus*, using the MASCOT algorithm embedded in BioTools software package (Bruker Daltonics). Dynamic oxidation of methionine and static carboxyamidomethylation of cysteine residues were set as modifications, trypsin was chosen as enzyme and two missed cleavages were allowed. The spectra were searched with a mass accuracy of 150 ppm and 0.7 Da for precursor and fragment ions, respectively. The Mascot results with a significance level over 95% ($p<0.05$) were accepted. The protein identifications were considered confident when, at least, a sequence coverage over 20% and a Mascot score ($p<0.05$) over 70 were reached. Most of the proteins have been identified in PMF MS scan mode.

2.5. Western blot validation

IPs from HT22 or Neuro-2a extracts obtained from a 70% confluent 10-cm dish as described in 2.2 were analyzed by 1D-

SDS-PAGE using the same parameters as described in 2.3. Proteins were transferred onto PVDF membranes (Millipore) and blots were blocked in TBS-Tween 0.05% containing 5% milk at room temperature for 1 h under shaking, and probed with anti-B-Raf, or anti-Hsp90, or anti-β-Actin, or anti-eIF4A1 (all these antibodies were from Santa Cruz Biotechnology), or anti-Hsc70 (Abcam), dissolved in the same blocking solution. Membranes were incubated with the corresponding secondary antibodies and proteins were visualized using an enhanced chemiluminescence system (ECL plus, Amersham Life Science). Immunoreactive signals were detected using light sensitive film (Fuji medical X-ray film). As a control a mock IP with normal rabbit IgG was carried out in parallel in all these experiments.

3. Results

3.1. *Isolation and identification of B-Raf interacting proteins*

HT22 mouse hippocampal cells were employed to isolate endogenous B-Raf-associated proteins by IP with a polyclonal antibody specific for this protein. To achieve greater specificity, we included a pre-clearing step using non-immune polyclonal antibodies generated in the same host species (rabbit) in which the B-Raf antibody was raised (Fig. 1A). Fig. 1B upper panel shows a western blot of resolved immunoprecipitates obtained with the anti B-Raf antibody and developed with the same antibody, verifying that the MAPKKK B-Raf was successfully immunoprecipitated from the cell lysates. The specificity of the IPs was assessed by developing the membrane with an antibody against the very abundant cytosolic protein GAPDH that is not expected to interact with B-Raf. GAPDH was detected in the input and output samples but was absent in the B-Raf and mock IPs (Fig. 1B lower panel). B-Raf immunoprecipitates were separated by one-dimensional gel electrophoresis and stained with Coomassie Brilliant Blue (Fig. 1C). The protein staining showed multiple bands suggesting the presence of a number of B-Raf interacting partners in the IPs.

For an exhaustive analysis of the isolated proteins, the SDS-PAGE gel lane was cut into 20 equal slices as indicated in Fig. 1C. Tryptic peptides prepared from each gel slice were separated by liquid chromatography (LC) prior to MALDI-MS/MS analysis. Separation at the peptide level resulted in the identification of different proteins from a single gel slice. Initially, all proteins from two independent experiments with a Mascot score higher than 40 and identified by at least two peptides were considered (Table 1). This table includes for each identified protein the associated peptide sequences with the respective information obtained from the Mascot database search. Then the cut-off criteria for the identity were established to have a False Discovery Rate (FDR) lower than 0.5% based on the search of a random mouse UniProt database. The Mascot score for the proteins was set to greater than 60, with two or more peptides identified per protein with a measured mass accuracy lower than 80 ppm (the overall mass accuracy average was 44 ppm), and having a Mascot score above 18. The FDR (%) was calculated as the ratio of the number of unique protein hits identified in the random database that surpassed the cut-off criteria and the protein hits identified in the forward database. The final list of proteins associated with B-Raf, identified under non-stimulating conditions from HT22 cells, is reported in Table 2. This list is the result from the overlap of the data generated from the two off-line LC-MALDI-MS/MS experiments. All these proteins identified surpassed the protein identification cut-off criteria including a 0.5% FDR value.

To analyze the phosphorylation state of the B-Raf interacting proteins under non-stimulating conditions, B-Raf immunoprecipitates were separated by 2D-PAGE and stained for the specific detection of phosphorylated proteins [32]. Protein spots visualized after ProQ staining (Supplementary Fig. 1) were excised from the gel and subjected to in-gel tryptic digestion prior to MALDI-MS/MS analysis. The protein identifications were considered confident when, at least, a sequence coverage over 20% and a Mascot score ($p<0.05$) over 70 were reached. Most of the proteins were identified in PMF MS scan mode. Significant hits ($p<0.05$) from MASCOT search results were taken as positive protein identification.

The final list of phosphorylated proteins associated with B-Raf in HT22 cells, identified under non-stimulating conditions, is reported in Table 3. As expected, the proteins identified with this approach represent a fraction of the total B-Raf interacting proteins detected after one-dimensional gel electrophoresis (Table 2).

3.2. *Confirmation of B-Raf interacting proteins by co-immunoprecipitation and western blot analysis*

We selected six proteins identified as B-Raf interactors, and confirmed these protein associations in non-stimulated HT22 cells using co-IPs and western blot. To make certain that the identified interacting partners were binding to B-Raf specifically, we performed parallel co-IPs in the cell lysate (mock IPs) using a polyclonal non-immune antibody from the same host specie in which the B-Raf antibody was raised (rabbit). In all cases, the amount of immunoprecipitated proteins with the non-specific antibody was considerably reduced or null compared to that obtained with the B-Raf antibody (Fig. 2: compare Mock and IP lanes). As shown in Fig. 2A, co-IP followed by western blot analysis validated the interaction of β-actin, HSP90, Hsc70 and eIF4A1 with B-Raf in HT22 cells.

To circumvent the problem of immunodetecting proteins that migrate close to IgG heavy chains during SDS-PAGE (as it is the case for vimentin and β-tubulin) we performed reciprocal IPs to validate B-Raf/vimentin and B-Raf/β-tubulin associations. Vimentin and β-tubulin IPs performed in cell lysates resolved by SDS-PAGE followed by B-Raf detection by western blot confirmed the interaction of both proteins with B-Raf (Fig. 2A).

To further extend these experiments, we studied the B-Raf interactors tested in HT22 cells in the Neuro-2a cells, a mouse neuroblastoma cell line derived from neural crest. Using the approach described above, we demonstrated that the B-Raf interactors validated in HT22 are not exclusive for this hippocampal cell line. As shown in Fig. 2B, in non-stimulated Neuro-2a cells, endogenous B-Raf was also specifically associated with β-actin, HSP90, Hsc70, eIF4A1, vimentin and β-tubulin.

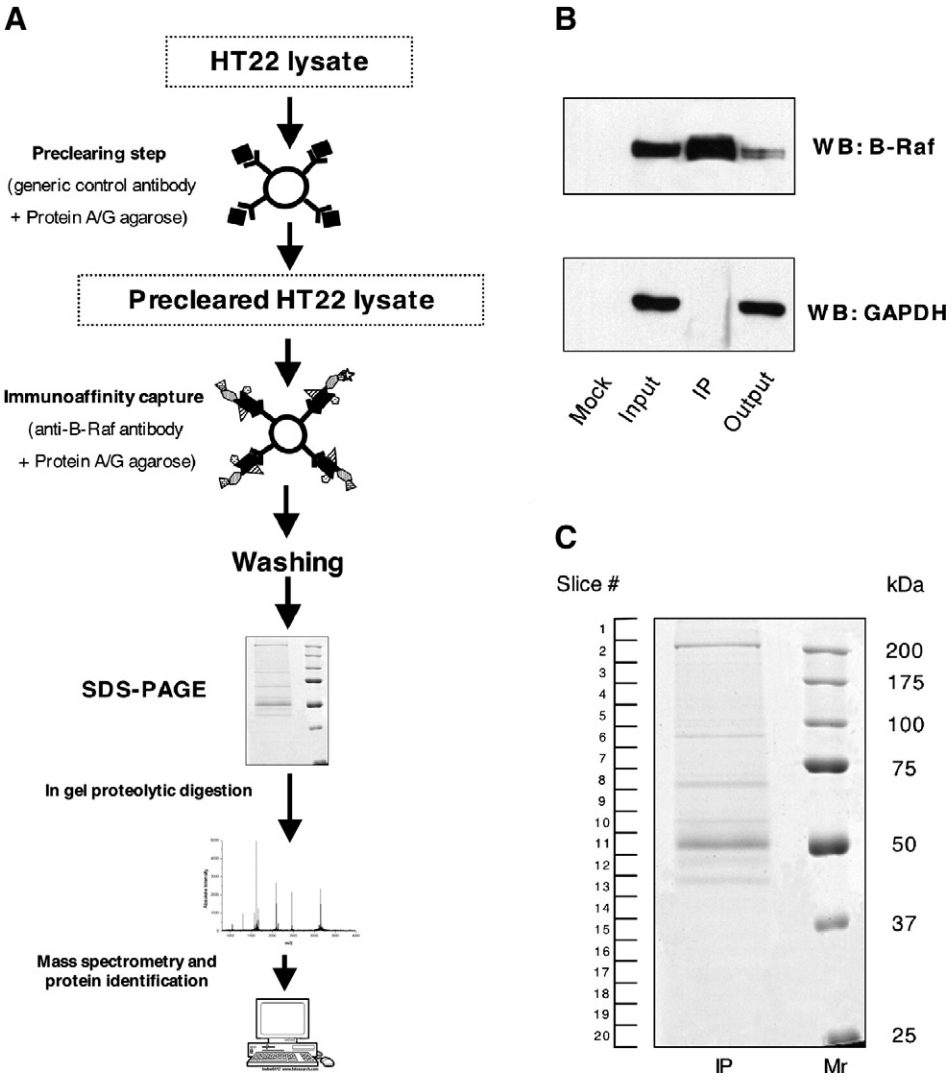

Fig. 1 – (A) Schematic representation of B-Raf co-IP experiment. HT22 lysate was initially incubated with a generic control antibody to perform a mock IP to reduce the number of non-specific proteins binding to B-Raf antibodies. After this pre-clearing step, anti-B-Raf antibody was added to the cell extract. Immunoprecipitates in both cases were collected using Protein A/G plus agarose. The captured complex containing the bait protein (B-Raf) was subjected to washing steps (PBS buffer) to reduce non-specific binders. Then the co-immunoprecipitated complex was resolved by SDS-PAGE and the gel lane was cut into 20 equal slices which were subsequently subjected to in-gel proteolytic digestion and analyzed by tandem MS (MALDI-MS/MS). The candidate interacting proteins were identified by querying the protein database with the mass spectrometry data. (B) Western blot confirms that B-Raf is present in immunoprecipitates obtained with the B-Raf antibody. Mock: IP performed in parallel with normal rabbit IgG. Input and output correspond to lysate samples before and after performing the IP, respectively. The PVDF membrane was probed with anti-B-Raf antibody (top panel) and with anti-GAPDH antibody (bottom panel). (C) Coomassie-stained 1D-SDS-PAGE gel illustrating the profile of proteins isolated by B-Raf IP from non-stimulated HT22 mouse hippocampal cells. The approximate molecular weights of the protein standards and gel slice regions are denoted on the right and left of the gel, respectively.

These results provide evidence that the identified proteins are B-Raf interactors in non-stimulated neurons.

4. Discussion

In this work, we have investigated the B-Raf interactome in neurons, using as model the hippocampal cell line HT22. The hippocampus is a brain structure involved in external environment processing, behavioral adaptation and memory formation. ERK1/2 signaling is implicated in molecular and cellular mechanisms important for hippocampal physiological function [17,18,33]. HT22 cells are a valuable tool to study molecular aspects of B-Raf activation since this kinase is expressed at high levels (Fig. 1) and ERK1/2 activation by stimuli such as oxidative stress has been extensively studied in this cell line [34,35].

Despite many recent reports based on the use of tagged proteins in the interactome mapping literature, there is a

Table 1 – List of murine proteins interacting with B-Raf identified by off-line LC-MALDI-MS/MS. [a]

Protein	UniProt accession number	MW [kDa]	Mascot score ($p<0.05$)	Seq. coverage [%]	Matched peptides	Slice #	MH+(calc) [Da]	Δm [Da]	Peptide ion score ($p<0.05$)	Sequence
B-Raf proto-oncogene serine/ threonine-protein kinase	P28028	90	241	12	3	6	1556.774	0.055	72	TPIQAGGYGEFAAFK
							1891.853	0.094	54	AGFQTEDFSLYACASPK
							2062.045	0.179	90	EQQLLESLVFQTPTDASR
Components of cytoeskeleton										
Myosin-9	Q8VDD5	227	957	12	16	2	1159.658	0.046	41	RGDLPFVVTR
							1193.616	0.087	26	ALELDSNLYR
							1318.748	0.079	39	LDPHLVLDQLR
							1524.806	0.053	36	TDLLLEPYNKYR
							1552.761	0.117	17	ITDVIIGFQACCR
							1558.859	0.074	55	QRYEILTPNSIPK
							1571.854	0.108	30	VSHLLGINVTDFTR
							1726.949	0.113	45	QLLQANPILEAFGNAK
							1815.908	0.117	105	IAQLEEQLDNETKER
							1869.966	0.126	47	ANLQIDQINTDLNLER
							1918.997	0.099	30	LQVELDSVTGLLSQSDSK
							1949.993	0.122	16	LQQELDDLLVDLDHQR
							1981.994	0.101	30	HSQAVEELADQLEQTKR
							1998.061	0.125	90	KANLQIDQINTDLNLER
							2333.056	0.181	58	MQQNIQELEEQLEEEESAR
							2472.174	0.17	166	IAQLEEELEEEQGNTELINDR
							2493.174	0.165	131	DFSALESQLQDTQELLQEENR
Myosin-10	Q61879	230	348	9	9	2	938.509	0.067	27	IVFQEFR
							1318.748	0.079	39	LDPHLVLDQLR
							1440.712	0.088	16	SDLLLEGFNNYR
							1663.817	0.008	34	ALEEALEAKEEFER
							1742.944	0.081	33	QLLQANPILESFGNAK
							1774.918	0.097	16	TTLQVDTLNTELAAER
							1799.913	0.008	21	IGQLEEQLEQEAKER
							1937.956	0.15	63	LQQELDDLTVDLDHQR
							2374.137	0.112	89	DAAGLESQLQDTQELLQEETR
Filamin-C	Q8VHX6	291	41	1	2	2	1400.648	0.056	23	YGGDEIPYSPFR
							1998.044	0.143	19	DVVDPGKVKCSGPGLGTGVR
Filamin-A	Q8BTM8	284	164	6	9	2	1379.674	0.046	17	YGGPYHIGGSPFK
							1400.648	0.056	52	YGGDEIPFSPYR
							1602.766	0.098	24	YNDQHIPGSPFTAR
							2467.189	0.169	22	FNEEHIPDSPFVVPVASPSGDAR
							2544.258	0.167	28	GLVEPVDVVDNADGTQTVNYVPSR
Vimentin	P20152	54	188	19	3	10	1527.828	0.061	47	HLREYQDLLNVK
							1838.961	0.039	22	ETNLESLPLVDTHSKR
							2377.166	0.288	96	QVQSLTCEVDALKGTNESLER
Tubulin beta-2C chain	P68372	50	56	7	2	10	1696.833	0.081	37	NSSYFVEWIPNNVK
							1843.934	0.086	19	INVYYNEATGGKYVPR
Tubulin beta-3 chain	Q9ERD7	51	63	9	3	10	1143.634	0.101	22	LAVNMVPFPR

(*continued on next page*)

Table 1 *(continued)*

Protein	UniProt accession number	MW [kDa]	Mascot score ($p<0.05$)	Seq. coverage [%]	Matched peptides	Slice #	MH+(calc) [Da]	Δm [Da]	Peptide ion score ($p<0.05$)	Sequence
							1958.982	0.03	30	GHYTEGAELVDSVLDVVR
Tubulin beta-5 chain	P99024	50	133	23	5	10	1143.634	0.101	22	LAVNMVPFPR
							1620.836	0.193	19	LHFFMPGFAPLTSR
							1958.982	0.03	30	GHYTEGAELVDSVLDVVR
							2798.343	0.174	33	SGPFGQIFRPDNFVFGQSGAGNNWAK
							3102.408	0.195	24	FWEVISDEHGIDPTGTYHGDSDLQLDR
Tubulin alpha-1B chain	P05213	51	204	28	8	10	1085.62	0.101	18	EIIDLVLDR
							1701.906	0.105	34	AVFVDLEPTVIDEVR
							1718.882	0.163	15	NLDIERPTYTNLNR
							1756.963	−0.027	20	IHFPLATYAPVISAEK
							2415.205	0.28	100	QLFHPEQLITGKEDAANNYAR
Tubulin alpha-1A chain	P68369	51	225	28	6	10	1085.62	0.101	18	EIIDLVLDR
							1598.767	0.024	22	TIQFVDWCPTGFK
							1701.906	0.105	34	AVFVDLEPTVIDEVR
							1718.882	0.163	15	NLDIERPTYTNLNR
							1756.963	−0.027	20	IHFPLATYAPVISAEK
							2415.205	0.28	100	QLFHPEQLITGKEDAANNYAR
Tubulin beta-6 chain	Q922F4	51	97	14	4	11	1143.634	0.003	35	LAVNMVPFPR
							1696.833	0.035	36	NSSYFVEWIPNNVK
							1958.982	0.073	22	GHYTEGAELVDSVLDVVR
Beta-actin-like protein 2	Q8BFZ3	42	250	17	3	13	1790.892	0.029	117	SYELPDGQVITIGNER
							1954.064	−0.053	74	VAPDEHPILLTEAPLNPK
							3183.614	−0.167	59	TTGIVMDSGDGVTHTVPIYEGYALPHAILR
Actin, cytoplasmic 1	P60710	42	393	26	5	13	1198.706	−0.022	43	AVFPSIVGRPR
							1790.892	0.029	117	SYELPDGQVITIGNER
							1954.064	−0.053	146	VAPEEHPVLLTEAPLNPK
							2231.065	0.059	29	DLYANTVLSGGTTMYPGIADR
							3183.614	−0.167	59	TTGIVMDSGDGVTHTVPIYEGYALPHAILR
Chaperones										
Heat shock protein HSP 90-alpha	P07901	85	148	7	3	6	1513.786	0.038	27	GVVDSEDLPLNISR
							1833.781	0.06	51	NPDDITNEEYGEFYK
Heat shock protein HSP 90-beta	P11499	84	331	11	3	6	1513.786	0.038	27	GVVDSEDLPLNISR
							1847.797	0.031	77	NPDDITQEEYGEFYK
							3535.645	−0.199	68	LGLGIDEDEVTAEEPSAAVPDEIPPLEGDEDASR
Stress-70 protein, mitochondrial	P38647	74	96	5	2	7	1694.85	0.078	52	NAVITVPAYFNDSQR
							2055.962	0.11	44	STNGDTFLGGEDFDQALLR

78 kDa glucose-regulated protein	P20029	72	156	10	3	7	1566.78	0.03	52	ITPSYVAFTPEGER
							1815.996	0.039	28	IINEPTAAAIAYGLDKR
							1887.971	0.041	72	VTHAVVTVPAYFNDAQR
Heat shock cognate 71 kDa protein	P63017	71	481	21	3	7	1787.99	0.029	35	IINEPTAAAIAYGLDKK
							1981.998	0.034	101	TVTNAVVTVPAYFNDSQR
							2774.327	0.03	24	QTQTFTTYSDNQPGVLIQVYEGER
60 kDa heat shock protein	P63038	61	177	6	2	9	1389.705	0.013	44	GYISPYFINTSK
							2560.249	0.092	133	LVQDVANNTNEEAGDGTTTATVLAR
mRNA metabolism and translation										
Nucleolin	P09405	77	65	5	2	4	1561.681	0.103	23	GFGFVDFNSEEDAK
							2214.041	0.09	42	GLSEDTTEETLKESFEGSVR
mRNA metabolism and translation										
Elongation factor 1-gamma	Q9D8N0	50	53	6	2	11	1241.652	0.014	21	STFVLDEFKR
							1707.871	0.024	32	VLSAPPHFHFGQTNR
Eukaryotic initiation factor 4A-I	P60843	46	84	6	2	12	1790.892	0.055	106	SYELPDGQVITIGNER
							1954.064	0.068	52	VAPDEHPILLTEAPLNPK
THO complex subunit 4	O08583	27	109	8	2	17	2034.973	0.034	71	QQLSAEELDAQLDAYNAR
							2364.143	−0.059	38	NSKQQLSAEELDAQLDAYNAR
Miscellaneous										
Fatty acid synthase	P19096	275	66	2	3	2	1497.697	0.053	35	FPQLDDTSFANSR
							1964.971	0.092	30	LFDHPEVPTPPESASVSR
Clathrin heavy chain 1	Q68FD5	193	158	7	8	3	1304.659	0.013	22	NNLAGAEELFAR
							1716.87	0.012	16	VSQPIEGHAASFAQFK
							1942.914	0.155	69	TSIDAYDNFDNISLAQR
							1971.029	0.147	21	LASTLVHLGEYQAAVDGAR
IgE-binding protein	P03975	63	44	3	2	4	1605.802	0.068	20	IQQAFPVFEGAEGGR
							1733.897	0.076	24	KIQQAFPVFEGAEGGR
E3 ubiquitin-protein ligase NEDD4	P46935	103	98	6	3	4	1585.87	0.007	33	LQNVAITGPAVPYSR
							2285.145	0.033	50	DDFLGQVDVPLYPLPTENPR
ATP synthase subunit beta	P56480	56	91	7	2	11	1919.096	0.021	24	VLDSGAPIKIPVGPETLGR
							1988.033	0.067	67	AIAELGIYPAVDPLDSTSR
Fructose-bisphosphate aldolase A	P05064	40	209	16	4	13	1342.711	−0.082	26	ADDGRPFPQVIK
							2258.036	−0.05	140	YTPSGQSGAAASESLFISNHAY
							2272.142	0.1	29	GVVPLAGTNGETTTQGLDGLSER

[a] This list of proteins associated to B-Raf, identified under non-stimulating conditions from HT22 cells, is the result of the data generated from two independent IPs and off-line LC-MALDI-MS/MS experiments. The table reports the protein name, the UniProt accession number (mouse database), the protein mass (kDa), the Mascot score and the gel slice from which these peptides were derived. For each protein, it is listed the number of matched peptides, the molecular weight (Da) of mono-charged peptide, the mass accuracy (Da), the scan mode and the peptide sequences. The Mascot score cut-off was set to 18 for peptide identification and to 40 for the protein identification. All proteins were identified from at least two peptides.

Table 2 – Identification of murine proteins interacting with B-Raf by off-line LC-MALDI-MS/MS. [a]

Protein	Entry name	UniProt accession number	MW [kDa]	Mascot score	Matched peptides	Slice #
Components of cytoskeleton						
Myosin-9	MYH9	Q8VDD5	227	957	16	2
Myosin-10	MYH10	Q61879	230	348	9	2
Tubulin alpha-1A chain	TBA1A	P68369	51	249	6	10
Tubulin beta-5 chain	TBB5	P99024	50	133	5	10
Vimentin	VIME	P20152	54	188	3	10
Actin, cytoplasmic 1	ACTB	P60710	42	393	5	13
Beta-actin-like protein 2	ACTBL	Q8BFZ3	42	250	3	13
Chaperones						
Heat shock protein HSP 90-beta	HS90B	P11499	84	331	3	6
Heat shock cognate 71 kDa protein	HSP7C	P63017	71	481	3	7
78 kDa glucose-regulated protein	GRP78	P20029	72	156	3	7
mRNA metabolism and translation						
Eukaryotic initiation factor 4A-I	IF4A1	P60843	46	84	2	12
THO complex subunit 4	THOC4	O08583	27	109	2	17

[a] The final list of proteins associated to B-Raf, identified under non-stimulating conditions from HT22 cells, is the result from the overlap of the data generated from two independent IPs and off-line LC-MALDI-MS/MS experiments. The table reports the protein name, the UniProt entry name and accession number (mouse database), the protein mass (kDa), the Mascot score, the number of the matched peptides and the gel slice from which these peptides were derived. The Mascot score cut-off was set to 18 for peptide identification and to 60 for protein identification. All proteins were identified from at least two peptides.

continued need for conventional co-IPs [25]. Several multi-protein complexes containing MAPKs, including B-Raf, have been identified using exogenous overexpression of epitope-tagged or fusion proteins [36,37]. Nevertheless protein interactions are significantly impacted by protein expression levels: false positive interactions are often detected when proteins are captured out of their authentic molecular environment. In the present work the B-Raf interactome was characterized under endogenous expression conditions, avoiding the problems encountered in overexpression studies.

The presence of some previously validated interactors [37–39] in our results serves as an internal validation of data quality whereas the confirmation of protein associations in another neuronal cell line (Neuro-2a) provides further evidence that the identified proteins are B-Raf interactors in neurons.

Contrary to previously reported works, our analysis was focused on describing the B-Raf interactome in a neuronal model and under non-stimulating conditions. Considering the high abundance of this kinase in the nervous system, identifying its partners in a neuronal cell line when the signal cascade is at a basal state serves as a good starting point for investigating different roles of these proteins that modulate the cascade.

The B-Raf interactome identified in this work is expected to result from a complex network of direct B-Raf interactors in concert with other numerous protein–protein associations. Grouped according to their functional categories, a large fraction of the identified proteins (7/12) are structural or accessory components of the cell cytoskeleton, whereas 3/12 are molecular chaperones, and 2/12 are involved in different aspects of mRNA metabolism and translation (Fig. 3 and Table 2). In the validation studies, we confirmed the interaction between B-Raf and proteins of the three functional categories: 3 components of cytoskeleton, 2 chaperones, and 1 protein involved in mRNA metabolism and translation. It is

Table 3 – List of murine phosphoproteins identified by 2DE gel ProQ staining and MALDI-MS/MS analysis. [a]

Protein	Entry name	UniProt accession number	MW [kDa]	Mascot score	Matched peptides	MS mode
Myosin-9	MYH9	Q8VDD5	227	73	5	PMF
Vimentin	VIME	P20152	54	157	26	PMF
Tubulin beta-5 chain	TBB5	P99024	50	88	12	PMF
Heat shock protein HSP 90-beta	HS90B	P11499	84	116	18	PMF
78 kDa glucose-regulated protein	GRP78	P20029	72	70	8	Lift

[a] The final list of phosphoproteins associated to B-Raf, identified under non-stimulating conditions from HT22 cells is the result from the overlap of the data generated from three independent IPs. The table reports the protein name, the UniProt entry name and accession number (mouse database), the protein mass (kDa), the Mascot score, the number of the matched peptides and the MS mode. The Mascot score cut-off was set to 70 for the protein identification. All proteins were identified from at least two peptides.

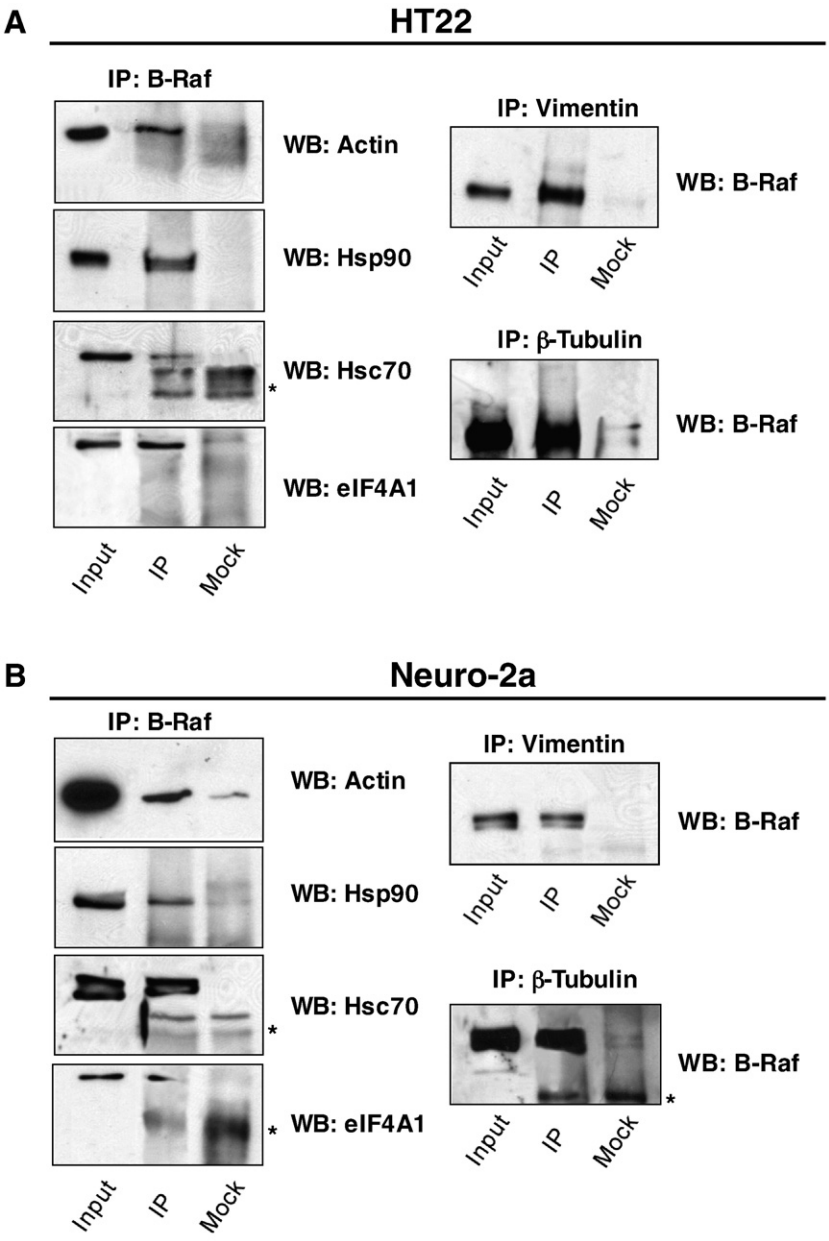

Fig. 2 – Validation of protein interactions by co-IP and western blot in HT22 (Panel A) and Neuro-2a (Panel B) cells. Western blot confirms that β-actin, Hsp90, Hsc70 and EIF4A1 are found in B-Raf immunoprecipitates. Reciprocal co-IP using anti-vimentin or anti-β-tubulin antibodies confirms the interaction of these proteins with B-Raf. Mock: IP performed in parallel with normal rabbit IgGs. IPs and western blots were performed with the indicated antibodies. *Region of the gel in lanes with samples containing immunoprecipitating antibodies that correspond to the running position of IgG chains.

interesting to note that in the full set of proteins identified (Table 1) 6 other components of cytoskeleton, 3 more chaperones, and 2 more mRNA metabolism and translation components were identified. Our protein identification criteria resulting in the 12 proteins listed in Table 2 were quite stringent. Emerging evidence indicates that, in response to stimuli, activation of signaling mediators, such as Raf kinases, requires assembled multiprotein complexes that sequester the protein in a spatiotemporal activatable state [1]. In agreement with this concept, and interestingly in the resting stage, we identified 10 (cytoskeleton and chaperones) B-Raf interacting partners that may function to assemble the B-Raf multimolecular complex that keeps B-Raf ready for activation in the HT22 cell line.

Molecular chaperones of the heat shock families Hsp70 and Hsp90 have been previously identified in association with B-Raf and other Raf kinases [37–39]. Cell fractionation and biochemical studies have identified B-Raf complexes containing Hsp90 in PC12 non-stimulated cells [40]. This highly stable association was found to be required to keep Raf proteins properly folded and soluble [41,42]. We identified two members of the Hsp70s interacting with B-Raf: the heat shock cognate 71 kDa protein (Hsc70; alternative names: Heat shock 70 kDa protein 8/Hspa8/Hsc70) and the 78 kDa glucose-

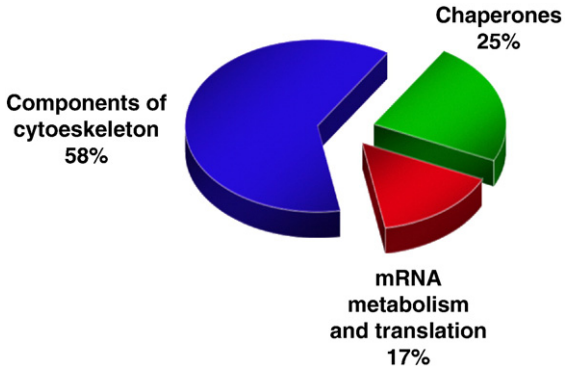

Fig. 3 – Pie chart of the identified B-Raf interacting proteins in HT22 cells under non-stimulating conditions, grouped according to their functional categories.

regulated protein (Heat shock 70 kDa protein 5/GRP78/Hspa5). A large number of protein interactions have been reported for Hsc70, including several of the proteins identified in this work (i.e. tubulin, actin, Hsp90). Although a long list of interacting partners is not surprising for Hsc70, a protein that is involved in assisting protein folding, it is noteworthy that this protein was identified in a number of projects defining interactions with signaling molecules. Hsc70 was identified as a β-arrestin interacting protein [43] and found in complexes with rhodopsin and guanylyl cyclase [44]. Recently, a constitutive association between B-Raf and Hsc70 was reported in HEK293 cells [37]. Hsc70 is highly expressed in the brain cytosol although it is able to associate with mitochondria to regulate protein transport, and was found involved in chaperone mediated autophagy, suggesting a role for this protein in neuronal survival in neurodegenerative processes [45,46].

B-Raf in non-stimulated cells is expected to be mainly in the cytosolic environment. However, we identified the abundant stress-regulated Hsp70 of the endoplasmic reticulum (Heat shock 70 kDa protein 5/GRP78) as a B-Raf interacting protein. A GRP78-Raf-1 interaction was recently reported, and proposed to be necessary to protect cells from endoplasmic reticulum stress-induced apoptosis [47]. This finding makes it unlikely that the association in the HT22 cell lysate is non-specific, and suggests a similar function performed by a GRP78-B-Raf association in cells in which this MAPKKK is expressed.

This is the first time that cytoskeleton structural components (actin and tubulin) and motor proteins (myosin) were identified in association with to a Raf kinase in general, and with B-Raf in particular. Evidence combining interactions of signaling molecules with the cytoskeleton, and the effects of drugs that alter cytoskeletal organization on signal transduction, reveal a critical role of these molecular components in the spatial organization of signaling complexes [48]. Based upon reported MEK and ERK binding to microtubules [49,50], B-Raf interaction with cytoskeleton components in non-stimulated cells may provide the platform that, together with scaffolding proteins, locates B-Raf into competent signaling complexes that will process the information of a particular activating stimulus.

The intermediate filament protein vimentin is a target of several kinases and is known to interact with a variety of cellular proteins, acting as a scaffold that modulates the transduction signal by MAPKs [51]. Vimentin and vimentin kinases were found associated with Raf-1 [52]. Our finding of an association of B-Raf with vimentin suggests that the regulation of ERK activity by vimentin may take place by similar mechanisms that involve association with members of the MAPKKK family.

The stringent conditions of the IPs were designed to avoid the risk of capturing non-specifically bound proteins to B-Raf. Under these conditions, some labile B-Raf interactions with true interacting partners could have been missed. For example, we did not identify members of the 14-3-3 signaling adaptor proteins in our work, although B-Raf-14-3-3 interaction has been described and analyzed in some detail [53,54]. Labile Raf-1 interactions have been reported: washing Raf-1 IPs with particular detergents removes 14-3-3 proteins, among other Raf-1 interacting partners [55,56]. Consistent with its high abundance in brain, 14-3-3 proteins are expressed at high levels in HT22 cells, and can be detected in B-Raf IPs from HT22 lysates prepared under milder conditions different than the ones used for the IPs in this work (data not shown).

The B-Raf-MEK-ERK signaling pathway controls many fundamental cellular processes including cell differentiation, proliferation, apoptosis and survival. Considering the fact that biomolecular interactions play a crucial role in the majority of cellular processes, identifying interactors of this MAPKKK as performed here, is a promising approach to discover key components with a critical function in the regulation of the B-Raf-MEK1/2-ERK1/2 signaling pathway, and shed light on the mechanisms of processing specific inputs into diverse biological responses triggered by the MAPK cascade in the nervous system.

Supplementary materials related to this article can be found online at doi:10.1016/j.jprot.2010.10.006.

Conflict of interest statement

The authors have declared no conflict of interest.

Acknowledgements

This work was supported by grants from the Agencia Nacional de Promoción Científica y Tecnológica (ANPCyT-Argentina, PICT-Max-Planck 06:205) to S.S. and C.W.T., and the Max Planck Society to C.W.T, G.M, F.H.

J.J.B. is a graduate student of Universidad de Buenos Aires. E.A. and S.S. are members of the Argentine National Research Council (CONICET).

REFERENCES

[1] Kolch W. Coordinating ERK/MAPK signalling through scaffolds and inhibitors. Nat Rev Mol Cell Biol 2005;6:827–37.
[2] Kolch W. Meaningful relationships: the regulation of the Ras/Raf/MEK/ERK pathway by protein interactions. Biochem J 2000;351(Pt 2):289–305.
[3] Morrison DK, Cutler RE. The complexity of Raf-1 regulation. Curr Opin Cell Biol 1997;9:174–9.

[4] Chong H, Vikis HG, Guan KL. Mechanisms of regulating the Raf kinase family. Cell Signal 2003;15:463–9.
[5] Wellbrock C, Karasarides M, Marais R. The RAF proteins take centre stage. Nat Rev Mol Cell Biol 2004;5:875–85.
[6] Pritchard CA, Samuels ML, Bosch E, McMahon M. Conditionally oncogenic forms of the A-Raf and B-Raf protein kinases display different biological and biochemical properties in NIH 3T3 cells. Mol Cell Biol 1995;15:6430–42.
[7] Marais R, Light Y, Paterson HF, Mason CS, Marshall CJ. Differential regulation of Raf-1, A-Raf, and B-Raf by oncogenic ras and tyrosine kinases. J Biol Chem 1997;272:4378–83.
[8] Jaiswal RK, Moodie SA, Wolfman A, Landreth GE. The mitogen-activated protein kinase cascade is activated by B-Raf in response to nerve growth factor through interaction with p21ras. Mol Cell Biol 1994;14:6944–53.
[9] Catling AD, Reuter CW, Cox ME, Parsons SJ, Weber MJ. Partial purification of a mitogen-activated protein kinase kinase activator from bovine brain. Identification as B-Raf or a B-Raf-associated activity. J Biol Chem 1994;269:30014–21.
[10] Moodie SA, Paris MJ, Kolch W, Wolfman A. Association of MEK1 with p21ras.GMPPNP is dependent on B-Raf. Mol Cell Biol 1994;14:7153–62.
[11] Reuter CW, Catling AD, Jelinek T, Weber MJ. Biochemical analysis of MEK activation in NIH3T3 fibroblasts. Identification of B-Raf and other activators. J Biol Chem 1995;270:7644–55.
[12] Huser M, Luckett J, Chiloeches A, Mercer K, Iwobi M, Giblett S, et al. MEK kinase activity is not necessary for Raf-1 function. EMBO J 2001;20:1940–51.
[13] Mikula M, Schreiber M, Husak Z, Kucerova L, Ruth J, Wieser R, et al. Embryonic lethality and fetal liver apoptosis in mice lacking the c-raf-1 gene. EMBO J 2001;20:1952–62.
[14] Mercer K, Chiloeches A, Huser M, Kiernan M, Marais R, Pritchard C. ERK signalling and oncogene transformation are not impaired in cells lacking A-Raf. Oncogene 2002;21:347–55.
[15] Wiese S, Pei G, Karch C, Troppmair J, Holtmann B, Rapp UR, et al. Specific function of B-Raf in mediating survival of embryonic motoneurons and sensory neurons. Nat Neurosci 2001;4:137–42.
[16] Vossler MR, Yao H, York RD, Pan MG, Rim CS, Stork PJ. cAMP activates MAP kinase and Elk-1 through a B-Raf- and Rap1-dependent pathway. Cell 1997;89:73–82.
[17] Arzt E, Holsboer F. CRF signaling: molecular specificity for drug targeting in the CNS. Trends Pharmacol Sci 2006;27: 531–8.
[18] Refojo D, Echenique C, Muller MB, Reul JM, Deussing JM, Wurst W, et al. Corticotropin-releasing hormone activates ERK1/2 MAPK in specific brain areas. Proc Natl Acad Sci USA 2005;102:6183–8.
[19] Silberstein S, Vogl AM, Refojo D, Senin SA, Wurst W, Holsboer F, et al. Amygdaloid pERK1/2 in corticotropin-releasing hormone overexpressing mice under basal and acute stress conditions. Neuroscience 2009;159:610–7.
[20] Mercer KE, Pritchard CA. Raf proteins and cancer: B-Raf is identified as a mutational target. Biochim Biophys Acta 2003;1653:25–40.
[21] Garnett MJ, Marais R. Guilty as charged: B-RAF is a human oncogene. Cancer Cell 2004;6:313–9.
[22] Wan PT, Garnett MJ, Roe SM, Lee S, Niculescu-Duvaz D, Good VM, et al. Mechanism of activation of the RAF-ERK signaling pathway by oncogenic mutations of B-RAF. Cell 2004;116: 855–67.
[23] Tran NH, Wu X, Frost JA. B-Raf and Raf-1 are regulated by distinct autoregulatory mechanisms. J Biol Chem 2005;280: 16244–53.
[24] Pandey A, Mann M. Proteomics to study genes and genomes. Nature 2000;405:837–46.
[25] Markham K, Bai Y, Schmitt-Ulms G. Co-immunoprecipitations revisited: an update on experimental concepts and their implementation for sensitive interactome investigations of endogenous proteins. Anal Bioanal Chem 2007;389:461–73.
[26] Gavin AC, Bosche M, Krause R, Grandi P, Marzioch M, Bauer A, et al. Functional organization of the yeast proteome by systematic analysis of protein complexes. Nature 2002;415: 141–7.
[27] Ho Y, Gruhler A, Heilbut A, Bader GD, Moore L, Adams SL, et al. Systematic identification of protein complexes in *Saccharomyces cerevisiae* by mass spectrometry. Nature 2002;415:180–3.
[28] Aebersold R, Mann M. Mass spectrometry-based proteomics. Nature 2003;422:198–207.
[29] Liu J, Li L, Suo WZ. HT22 hippocampal neuronal cell line possesses functional cholinergic properties. Life Sci 2009;84: 267–71.
[30] Perkins DN, Pappin DJ, Creasy DM, Cottrell JS. Probability-based protein identification by searching sequence databases using mass spectrometry data. Electrophoresis 1999;20:3551–67.
[31] Kronsbein HC, Jastorff AM, Maccarrone G, Stalla G, Wurst W, Holsboer F, et al. CRHR1-dependent effects on protein expression and posttranslational modification in AtT-20 cells. Mol Cell Endocrinol 2008;292:1–10.
[32] Jacob AM, Turck CW. Detection of post-translational modifications by fluorescent staining of two-dimensional gels. Meth Mol Biol 2008;446:21–32.
[33] Sweatt JD. Mitogen-activated protein kinases in synaptic plasticity and memory. Curr Opin Neurobiol 2004;14:311–7.
[34] Luo Y, DeFranco DB. Opposing roles for ERK1/2 in neuronal oxidative toxicity: distinct mechanisms of ERK1/2 action at early versus late phases of oxidative stress. J Biol Chem 2006;281:16436–42.
[35] Stanciu M, Wang Y, Kentor R, Burke N, Watkins S, Kress G, et al. Persistent activation of ERK contributes to glutamate-induced oxidative toxicity in a neuronal cell line and primary cortical neuron cultures. J Biol Chem 2000;275: 12200–6.
[36] Papin C, Denouel A, Calothy G, Eychene A. Identification of signalling proteins interacting with B-Raf in the yeast two-hybrid system. Oncogene 1996;12:2213–21.
[37] Gloeckner CJ, Boldt K, Schumacher A, Roepman R, Ueffing M. A novel tandem affinity purification strategy for the efficient isolation and characterisation of native protein complexes. Proteomics 2007;7:4228–34.
[38] Fischer A, Baljuls A, Reinders J, Nekhoroshkova E, Sibilski C, Metz R, et al. Regulation of RAF activity by 14-3-3 proteins: RAF kinases associate functionally with both homo- and heterodimeric forms of 14-3-3 proteins. J Biol Chem 2009;284: 3183–94.
[39] Zhu J, Balan V, Bronisz A, Balan K, Sun H, Leicht DT, et al. Identification of Raf-1S471 as a novel phosphorylation site critical for Raf-1 and B-Raf kinase activities and for MEK binding. Mol Biol Cell 2005;16:4733–44.
[40] Jaiswal RK, Weissinger E, Kolch W, Landreth GE. Nerve growth factor-mediated activation of the mitogen-activated protein (MAP) kinase cascade involves a signaling complex containing B-Raf and HSP90. J Biol Chem 1996;271: 23626–9.
[41] Schulte TW, Blagosklonny MV, Ingui C, Neckers L. Disruption of the Raf-1-Hsp90 molecular complex results in destabilization of Raf-1 and loss of Raf-1-Ras association. J Biol Chem 1995;270:24585–8.
[42] Schulte TW, Blagosklonny MV, Romanova L, Mushinski JF, Monia BP, Johnston JF, et al. Destabilization of Raf-1 by geldanamycin leads to disruption of the Raf-1-MEK-mitogen-activated protein kinase signalling pathway. Mol Cell Biol 1996;16:5839–45.
[43] Xiao K, McClatchy DB, Shukla AK, Zhao Y, Chen M, Shenoy SK, et al. Functional specialization of beta-arrestin interactions

revealed by proteomic analysis. Proc Natl Acad Sci USA 2007;104:12011–6.
[44] Bhowmick R, Li M, Sun J, Baker SA, Insinna C, Besharse JC. Photoreceptor IFT complexes containing chaperones, guanylyl cyclase 1 and rhodopsin. Traffic 2009;10:648–63.
[45] Johnson F, Kaplitt MG. Novel mitochondrial substrates of omi indicate a new regulatory role in neurodegenerative disorders. PLoS ONE 2009;4:e7100.
[46] Yang Q, She H, Gearing M, Colla E, Lee M, Shacka JJ, et al. Regulation of neuronal survival factor MEF2D by chaperone-mediated autophagy. Science 2009;323:124–7.
[47] Shu CW, Sun FC, Cho JH, Lin CC, Liu PF, Chen PY, et al. GRP78 and Raf-1 cooperatively confer resistance to endoplasmic reticulum stress-induced apoptosis. J Cell Physiol 2008;215: 627–35.
[48] Gundersen GG, Cook TA. Microtubules and signal transduction. Curr Opin Cell Biol 1999;11:81–94.
[49] Reszka AA, Seger R, Diltz CD, Krebs EG, Fischer EH. Association of mitogen-activated protein kinase with the microtubule cytoskeleton. Proc Natl Acad Sci USA 1995;92: 8881–5.
[50] MacCormick M, Moderscheim T, van der Salm LW, Moore A, Pryor SC, McCaffrey G, et al. Distinct signalling particles containing ERK/MEK and B-Raf in PC12 cells. Biochem J 2005;387:155–64.
[51] Ivaska J, Pallari HM, Nevo J, Eriksson JE. Novel functions of vimentin in cell adhesion, migration, and signaling. Exp Cell Res 2007;313:2050–62.
[52] Janosch P, Kieser A, Eulitz M, Lovric J, Sauer G, Reichert M, et al. The Raf-1 kinase associates with vimentin kinases and regulates the structure of vimentin filaments. FASEB J 2000;14:2008–21.
[53] Qiu W, Zhuang S, von Lintig FC, Boss GR, Pilz RB. Cell type-specific regulation of B-Raf kinase by cAMP and 14-3-3 proteins. J Biol Chem 2000;275:31921–9.
[54] Yamamori B, Kuroda S, Shimizu K, Fukui K, Ohtsuka T, Takai Y. Purification of a Ras-dependent mitogen-activated protein kinase kinase kinase from bovine brain cytosol and its identification as a complex of B-Raf and 14-3-3 proteins. J Biol Chem 1995;270:11723–6.
[55] Janosch P, Schellerer M, Seitz T, Reim P, Eulitz M, Brielmeier M, et al. Characterization of IkappaB kinases. IkappaB-alpha is not phosphorylated by Raf-1 or protein kinase C isozymes, but is a casein kinase II substrate. J Biol Chem 1996;271: 13868–74.
[56] Michaud NR, Fabian JR, Mathes KD, Morrison DK. 14-3-3 is not essential for Raf-1 function: identification of Raf-1 proteins that are biologically activated in a 14-3-3- and Ras-independent manner. Mol Cell Biol 1995;15: 3390–7.